Int. J. Electrochem. Sci., 13 **(2018)** 4741 – 4752, doi; 10.20964/2018.05.59

International Journal of ELECTROCHEMICAL SCIENCE
www.electrochemsci.org

Fabrication of an Electrochemical Biosensor Based on Nafion/Horseradish Peroxidase/Co_3O_4 NP/CILE and Its Electrocatalysis

Wei Chen[1], *Wenju Weng*[1], *Chunxiao Yin*[1], *Xueliang Niu*[2], *Guangjiu Li*[1,*], *Hui Xie*[2], *Juan Liu*[1], *Wei Sun*[2]

[1] Key Laboratory of Sensor Analysis of Tumor Marker, Ministry of Education, College of Chemistry and Molecular Engineering, Qingdao University of Science and Technology, Qingdao 266042, P R China
[2] Key Laboratory of Functional Materials and Photoelectrochemistry of Haikou, College of Chemistry and Chemical Engineering, Hainan Normal University, Haikou 571158, P R China
[*]E-mail: lgjqust@126.com

Received: 17 January 2018 / *Accepted:* 9 March 2018 / *Published:* 10 April 2018

This paper focuses on the investigation of direct electrochemistry and electrocatalysis of horseradish peroxidase (HRP) on Co_3O_4 nanoparticles (NPs) decorated carbon ionic liquid electrode (CILE) as an electrochemical biosensor for determinations of trichloroacetic acid (TCA) and sodium nitrite ($NaNO_2$). Co_3O_4 NPs were served to bridge the gaps between electron transport of electrochemical active site of HRP to the electrode with the ability to enhance the loading capacity of HRP on the electrode. Various material characterization techniques such as scanning electron microscopy, transmission electron microscopy, Raman and X-ray photoelectron spectroscopy were used to check the structure, morphology and crystal form of Co_3O_4 NP. Spectroscopic data testified that no denaturation occurred in the structure of HRP. Electrochemical performances of Nafion/HRP/Co_3O_4/CILE were conducted in pH 3.0 phosphate buffer solutions, which indicated that electron communication was achieved with the appearance of one well-distinct peak couple. Low detection limits and wide linear ranges were obtained in electrocatalytic investigations for the different substrates including TCA and $NaNO_2$ with the real samples detected successfully.

Keywords: Carbon ionic liquid electrode; direct electron transfer; Co_3O_4 nanoparticles; horseradish peroxidase; electrocatalysis.

1. INTRODUCTION

Electrochemical biosensors, which act as a kind of instrument that can switch concentration information into electrical signals, are very sensitive to bio-active substances and have been widely

explored due to their distinct advantages such as high sensitivity and accuracy, fast response, excellent selectivity. The applications involve many fields such as cancer diagnosis, water analysis, heavy metal ions detection and toxicity detection [1-4]. Various materials such as metal-organic frameworks [5], metallic oxides [6], transitional metal dichalcogenides [7], carbon derivatives [8], graphene (GR) and its derivatives [9-12] have been used for the preparations of biosensors. As a commonly used metal oxide, nanosized Co_3O_4 possesses some superiority, including excellent reversible redox ability, large specific area, semiconductivity, great catalytic performance, long service life and good corrosion resistance. Bao prepared a three-dimensional (3D) GR frameworks/Co_3O_4 composites electrode to detect glucose [13]. Yu designed a sensor for detecting lead ions by electrodeposition and annealing of Co_3O_4 nanosheets on indium tin oxide substrate electrode [14]. Dhas deposited porous Co_3O_4 films by nebulizer spray technique and applied to electrochemical sensing of glucose [15]. Song fabricated a 3D electrode by forming Co_3O_4 nanosheets on reduced graphene oxide modified Ni foam for electroreduction of H_2O_2 [16]. Cui applied mesoporous Co_3O_4 modified glassy carbon electrode (GCE) to simultaneously detect hydroquinone and catechol [17].

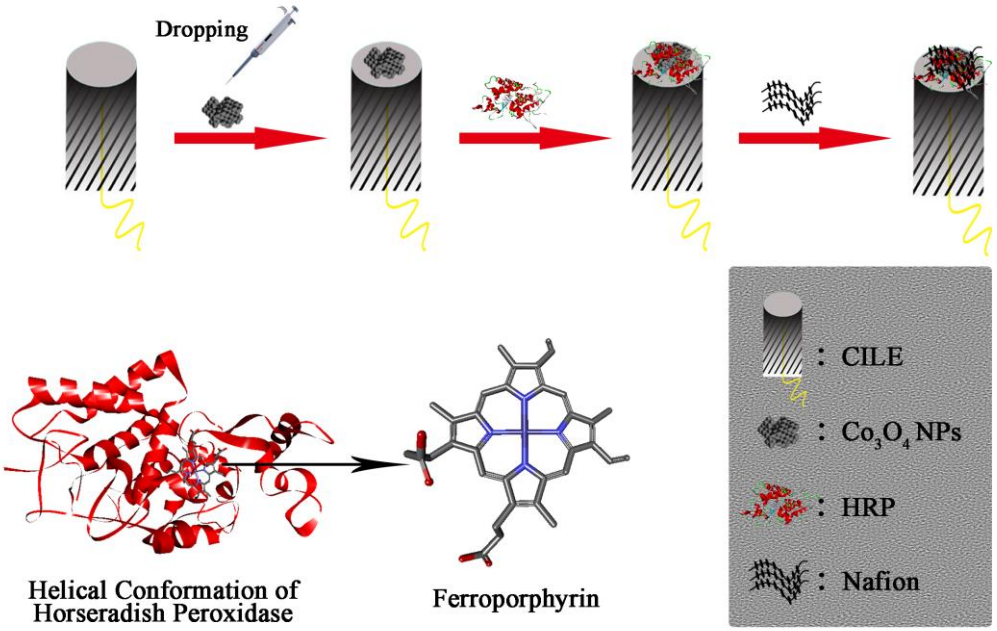

Scheme 1. Flowchart of this electrochemical biosensor fabrication and helical conformation of HRP with ferroporphyrin buried.

As a typical redox enzyme, horseradish peroxidase (HRP) has gained much attention in biosensing. However, electrochemical active centers of HRP are buried deeply in proteins or enzymes, which results in the difficulty for the electron transfer. Many nanomaterials have been explored to establish the electron transfer bridge for electron communication. Liu designed a H_2O_2 biosensor based on a Nafion/HRP/3DBi_2WO_6/GCE [18]. Mohammad fabricated an amperometric biosensor by decorating HRP on acrylic microspheres for the detection of capsaicin [19]. An enzymatic biosensor that aimed at the simultaneous determination of butylated hydroxyanisole and propyl gallate was

reported on Au-Pt nanotube/Au-GR immobilized with HRP [20]. Liu proposed an electrochemical method for detecting H_2O_2 in living cells with porous GR and HRP [21]. Ren constructed a cellular H_2O_2 ultramicrobiosensor by utilizing HRP, 1-butyl-3-methylimidazolium tetrafluoroborate and single-walled carbon nanotubes for real-time determination in vitro [22].

In this paper, Co_3O_4 NPs were characterized by various techniques such as SEM, TEM, Raman and XPS, which was farther modified on the electrode surface. HRP was immobilized on Co_3O_4 modified electrode and direct electrochemistry of HRP was investigated. Electrocatalytic behaviors of HRP towards TCA and $NaNO_2$ were checked in detail by cyclic voltammetry, and various samples were detected by this proposed method with satisfactory results. The fabrication procedure of this HRP-Co_3O_4 NPs based electrode was depicted in the following scheme 1.

2. MATERIALS AND METHODS

2.1 Instruments

CHI 604E electrochemical workstation (Shanghai CH Instrument, China) was used for electrochemical experiments, which was connected with a modified electrode (Φ = 4.0 mm) as working electrode, a platinum wire electrode as auxiliary electrode and a saturated calomel electrode (SCE) as reference electrode. Scanning electron microscopy (SEM) was performed on a JSM-7100F scanning electron microscope (JEOL, Japan) with transmission electron microscopy (TEM) on a JEM2010F transmission electron microscope (JEOL, Japan). Fourier transform infrared (FT-IR) spectrum and ultraviolet-visible (UV-Vis) absorption spectrum were performed on Nicolet 6700 FT-IR spectrometer (Thermo Fisher Scientific Inc., USA) and TU-1901 double-beam UV-visible spectrophotometer (Beijing Purkinje General Instrument Co., Ltd., China), respectively. Raman spectrum was obtained on a LabRAM HR system using 532 nm lasers (Horiba, France) and X-ray photoelectron spectroscopy (XPS) was on an AXIS HIS 165 spectrometer (Kratos Analytical, UK).

2.2 Reagents

1-Hexylpyridinium hexafluorophosphate ($HPPF_6$, Lanzhou Yulu Fine Chem. Ltd. Co., China), Co_3O_4 NPs ((Nanjing XFNANO Materials Tech. Ltd. Co., China), graphite powder (average particle size 30 μm, Shanghai Colloid Chemical Co., China), HRP (MW. 40000, Sinopharm Chem. Reagent Co., China), trichloroacetic acid (TCA, Tianjin Kemiou Chem. Co., China) and $NaNO_2$ (Shanghai Chem. Plant, China) were used as received. 0.1 mol·L^{-1} phosphate buffer solution (PBS) were selected as the supporting electrolyte. All other chemicals were of analytical grade and used directly.

2.3 Fabrications of Nafion/HRP/Co_3O_4/CILE

Based on the procedure of the former report [23], CILE was prepared with graphite power and $HPPF_6$ (at the mass ratio of 2:1) into a glass electrode tube (Φ = 4 mm), which were utilized as

substrate electrode and compacted with the surface smoothed before each usage. Afterwards CILEs were decorated with 6.0 μL of 0.5 $mg \cdot mL^{-1}$ Co_3O_4 NPs suspension solution, 8.0 μL of 15.0 $mg \cdot mL^{-1}$ HRP solution and 6 μL of 0.5% Nafion solution by direct dropping step-by-step and dried after each step, which was denoted as Nafion/HRP/Co_3O_4/CILE. Other similar modified electrodes like Nafion/CILE, Nafion/HRP/CILE and Nafion/Co_3O_4/CILE were fabricated as well for experimental comparisons.

2.4 Procedure

All the electrochemical experiments were performed in a 10 mL electrochemical cell with 0.1 $mol \cdot L^{-1}$ PBS at the ambient temperature (20±2℃), which was deoxygenized by N_2 for 30 min just before each experiment in order to keep the micro-environment without oxygen. UV-Vis spectroscopy was conducted with HRP-Co_3O_4 mixture in pH 3.0 PBS. The HRP-Co_3O_4 mixture was dropped onto a slide glass and dried for FT-IR experiment.

3. RESULTS AND DISCUSSION

3.1 Characterizations of Co_3O_4 NPs

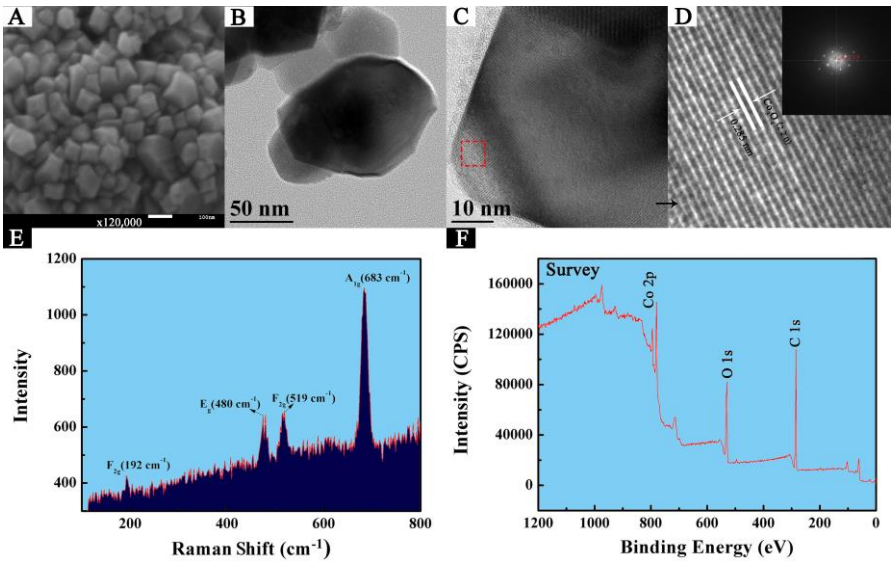

Figure 1. Structural and morphological characterizations of Co_3O_4 NPs: (A) SEM image; (B) TEM image; (C and D) HR-TEM (insert is fast-Fourier transform electron diffraction pattern); (E) Raman spectrum; (F) XPS spectrum.

SEM image of Co_3O_4 NP used was present as in Fig.1A, which had many spinel-shaped nanoparticles aggregated together. TEM image (Fig.1B) exhibited the typical structure of Co_3O_4 NPs with the average diameter of 50 nm. Fig.1C and D gave HR-TEM images of Co_3O_4 NPs, which also presented the distinct spinel-structure. The fast-Fourier transform electron diffraction pattern (insert in

Fig.1D) revealed that Co_3O_4 NPs mainly belongs to {220} crystal form according to its lattice fringe separation as 0.285 nm [24]. Fig.1E depicted the Raman spectrum of Co_3O_4 NPs and four Raman bands locating at 192, 480, 519 and 683 cm^{-1} could be all detected, which was corresponding to Raman active E_g and A_{1g}. The results were close to the data of standard Co_3O_4 micro-crystal and demonstrated the existence of spinel morphology [25]. On XPS spectrum (Fig.1F) the dominant peaks were distinctly indexed as Co 2p, O 1s, and C 1s regions, suggesting no other existence of metallic or inorganic substances [26].

3.2 Spectroscopic results

UV-Vis absorption spectrum can be used to observe the secondary biological structure of the proteins or enzymes and the shifting of the typical Soret band can give the structural information [27]. Fig.2A depicted the UV-Vis spectra of HRP (curve a) and HRP-Co_3O_4 mixture in pH 3.0 PBS (curve b), which gave the same typical Soret band at 403.00 nm. Therefore the biostructure of HRP remained the changeless after mixing with Co_3O_4 NPs in pH 3.0 PBS. FT-IR spectroscopy is generally utilized to monitor the secondary structure of polypeptide chain of enzymes [28]. The amide I and II bands of the pure HRP appears at 1640 and 1540 cm^{-1} (curve a of Fig.2B), where the peak that locates around 1700-1600 cm^{-1} is attributed to C=O stretching vibrations and the peak around 1600-1500 cm^{-1} results from the combination of both N-H bending and C-N stretching in the groups. As shown in Fig.2B, FT-IR spectrum of HRP-Co_3O_4 composite film appeared at 1650 cm^{-1} and 1540 cm^{-1} (curve b), which was similar to that of HRP (curve a). Therefore HRP held its original structure after blending with Co_3O_4 NPs with the fundamental active conformation of HRP remained.

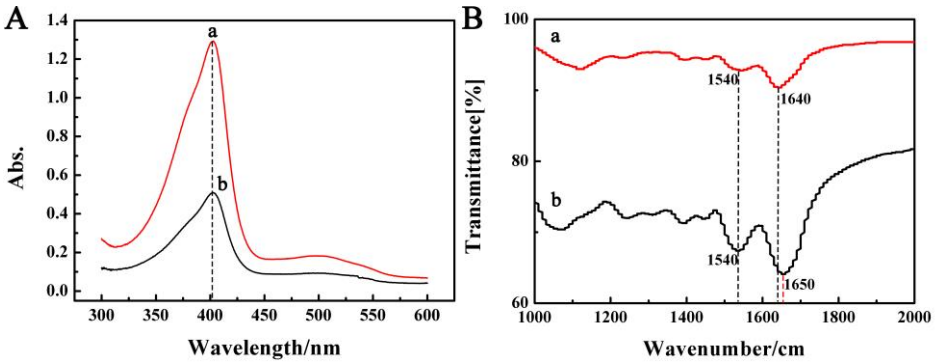

Figure 2. UV-Vis absorption spectra of HRP (a) and HRP-Co_3O_4 mixture (b) in pH 3.0 PBS; (B) FT-IR spectra of HRP (a) and HRP-Co_3O_4 composite film (b).

3.3 Direct electrochemical behaviors

Cyclic voltammograms of different modified electrodes were investigated with the curves described in Fig.3. There is no redox peaks appeared on Nafion/CILE (a) and Nafion/Co_3O_4/CILE (b), suggesting that no electrochemical reactions took place. On Nafion/HRP/CILE (curve c) a pair of asymmetrical redox couple appeared, indicating that electron transfer of HRP was achieved. The result

was in good agreement with the former report, which exhibited the specific interfacial properties of CILE for electron transfer [29]. On Nafion/HRP/Co_3O_4/CILE (curve d) the redox peak current increased with a well-distinct symmetrical redox couple observed, which was attributed to the existence of Co_3O_4 NPs that facilitated electron transfer rate and enhanced the loading capacity of HRP on the substrate electrode surface. Co_3O_4 NPs possess many physicochemical properties including good biocompatibility, interfacial hydrophilicity and small surface area, of which the ability are widely shown to fasten the electron transfer and served as electron bridges. The cathodic (Epc) and anodic (Epa) peak potentials were observed at -0.114 V and -0.177 V (vs. SCE) with the formal potential ($E^{0'}$) calculated as -0.146 V (*vs*. SCE), which was the typical redox couple of Fe(Ⅲ)/Fe(Ⅱ) in ferriporphyrins [30]. The ratio of redox currents was approximation as 1.0 with the peak-to-peak potential separation (ΔEp) as 66 mV, proving that it was a quasi-reversible electrochemical procedure.

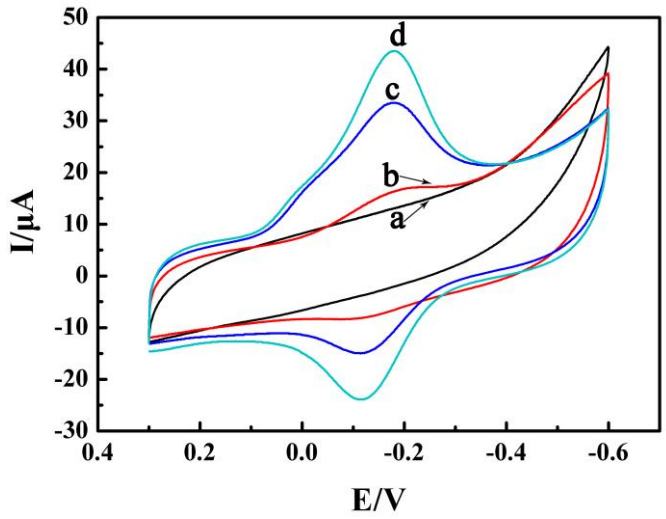

Figure 3. CVs of Nafion/CILE (a), Nafion/Co_3O_4/CILE (b), Nafion/HRP/CILE (c) and Nafion/HRP/Co_3O_4//CILE (d) in pH 3.0 PBS with scan rate of 0.1 V·s^{-1}.

3.4 Electrochemical investigations

Effects of scan rate on cyclic voltammetric responses of Nafion/HRP/Co_3O_4/CILE were explored in pH 3.0 PBS from 0.03 to 1.00 V·s^{-1} with the curves displayed in Fig.4A. The redox peak potentials moved slightly towards positive and negative terminals respectively with the growth of scan rate, and the increase of ΔEp value took place simultaneously, suggesting that the electron transfer became more quasi-reversible at faster scan rate. Also the signals of redox couple augmented gradually along with the increasing scan rate, demonstrating that HRP underwent a characteristic interface-controlled process. Two linear regression equations of redox currents versus scan rate (Fig.4B) were obtained as Ipc (μA) = 107.1 υ (V·s^{-1}) - 5.24 (n=10, γ=0.994) and Ipa (μA) = -105.1 υ (V·s^{-1}) - 10.08 (n=10, γ=0.997). The relationships of redox potentials versus logυ were plotted and the regression equations (Fig.4C) were computed as Epc (V) = -0.068 logυ (V·s^{-1}) - 0.31 (n=8, γ=0.995) and Epa (V) = 0.057 logυ (V·s^{-1}) - 0.072 (n=8, γ=0.993). Therefore the electron transfer number (*n*), charge transfer

coefficient (α) and the apparent heterogeneous electron transfer rate constant (k_s) were obtained as 0.83, 0.46 and 0.94 s^{-1} based on the Equations shown below, respectively. So the presence of Co_3O_4 NPs could build a favorable microplatform to facilitate electron communication of ferriporphyrins.

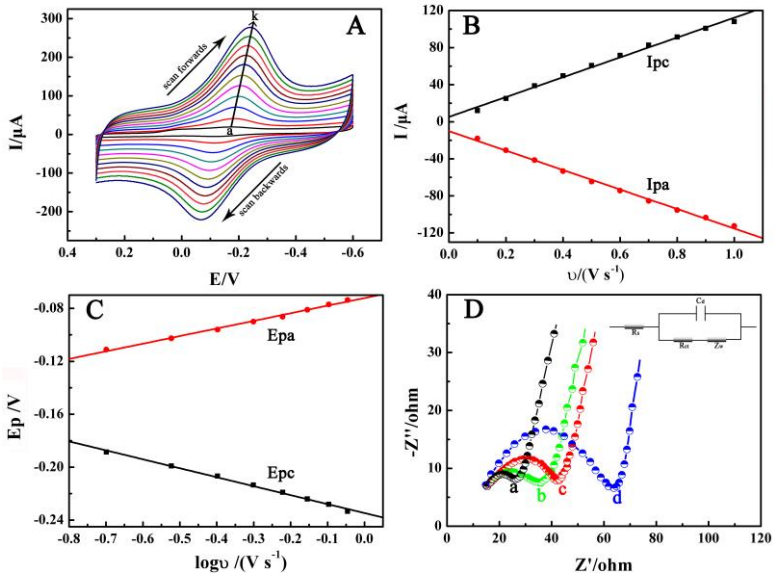

Figure 4. (A) CVs of Nafion/HRP/Co_3O_4/CILE swept at different scan rates (from a to k as 30, 100, 200, 300, 400, 500, 600, 700, 800, 900, 1000 $mV \cdot s^{-1}$) in pH 3.0 PBS; (B) Linear relationship of the redox currents *vs* scan rate (υ); (C) Linear relationship of the redox peak potentials *vs* logυ; (D) EIS pattern of Nafion/Co_3O_4/CILE (a), Nafion/HRP/Co_3O_4/CILE (b), Nafion/CILE (c) and Nafion/HRP/CILE (d) in a 10.0 $mmol \cdot L^{-1}$ $[Fe(CN)_6]^{3-/4-}$ and 0.1 $mol \cdot L^{-1}$ KCl solution with frequency from 10^4 to 0.1 Hz (Inset is the Randles circuit model in the cell).

Moreover, the apparent surface concentration (Γ*) of HRP is obtained by Faraday's equation: $Q=nFA\Gamma$* [31], of which Q is for the quantity of electricity, n is for electron transfer number, F is for Faraday's constant, A is for geometric area of this biosensor. Then the Γ* of HRP on Nafion/HRP/Co_3O_4/CILE was reckoned as 1.61×10^{-9} $mol \cdot cm^{-2}$, holding the proportion of 6.74% HRP that loaded on the electrode surface (2.39×10^{-8} mol cm^{-2}). Therefore Co_3O_4 NPs provided more chances for electron transfer inside the enzyme.

$$E_{pa} = E^{0'} + \frac{RT}{(1-\alpha)nF}\ln\upsilon \quad (1)$$

$$E_{pc} = E^{0'} - \frac{RT}{\alpha nF}\ln\upsilon \quad (2)$$

$$\log k_s = \alpha\log(1-\alpha) + (1-\alpha)\log\alpha - \log\frac{RT}{nF\upsilon} - (1-\alpha)\alpha\frac{nF\Delta E_p}{2.3RT} \quad (3)$$

Electrochemical impedance spectroscopic (EIS) results were depicted in Fig.4D, and the electron transfer resistance (Ret) value can reflect the conductivity of materials on the interface [32]. The Ret of Nafion/CILE was got as 56.5 Ω (curve c), and the loading of Co_3O_4 NPs and HRP on the electrode surface gave the Ret values of 25.0 Ω (curve a) and 88.1 Ω (curve d), indicating that Co_3O_4

NPs and HRP had different influences on the interfacial resistances. As for Nafion/HRP/Co_3O_4/CILE (curve b), the Ret value was reckoned as 36.2 Ω, which was in the middle of Nafion/Co_3O_4/CILE and Nafion/HRP/CILE, demonstrating that the synergistic effects between Co_3O_4 NPs and HRP on the electrode surface.

3.5 Influence of electrolyte pH

Electrochemical behaviors of enzyme can be tremendously influenced by the pH environment of electrolyte and the relationship between $E^{0'}$ versus pH can provide the information of electrochemical process. Effect of pH on cyclic voltammetric responses of Nafion/HRP/Co_3O_4/CILE was analysed with the data shown in Fig.5A. The $E^{0'}$ value moved towards negative terminal with electrolyte pH increasing. The linear regression equation was computed as $E^{0'}$ (V)=-0.0606pH + 0.033 (n=5, γ=0.999) with the slope as -60.6 mV·pH^{-1}, which was almost the same as that of the theoretical one (-59.0 mV·pH^{-1}) at 298 K for reversible process [33]. The result demonstrated that HRP was in accord with the one-protonation process along with one-electron transferring to electrode surface, which could be shown as following equation: HRP Fe(III) + H^+ + e^- $\rightleftharpoons$ HRP Fe(II) [34]. And the highest response was observed at pH 3.0 and chosen to be the supporting electrolyte because more protons could be provided for electrode reaction.

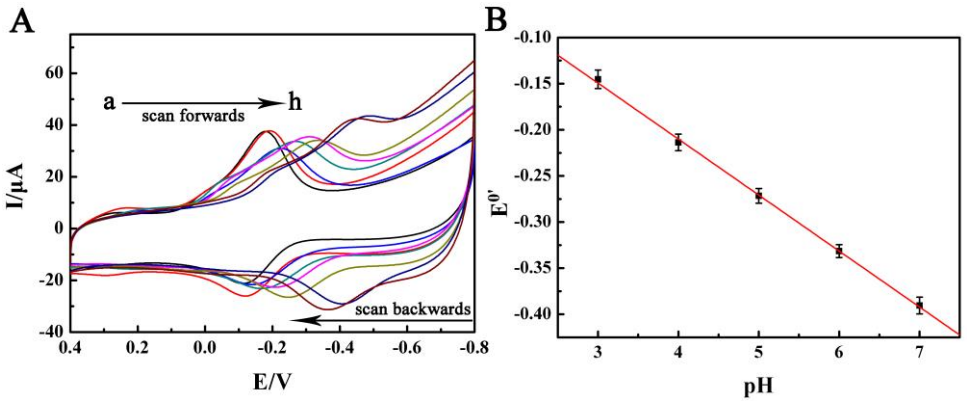

Figure 5. (A) Influence of electrolyte pH on Nafion/HRP/Co_3O_4/CILE at the scan rate of 0.1 V·s^{-1} (from a to h as 2.0, 3.0, 4.0, 5.0, 6.0, 7.0, 8.0, 9.0); (B) Linear relationship of $E^{0'}$ versus pH.

3.6 Electrocatalysis performances

HRP based electrodes exhibit excellent electrocatalytic effects due to its specific enzyme structure. Therefore the electrocatalysis performances to various substrates were checked in detail. As an organic halide, TCA is widely used as a herbicide in the field of agriculture, and it also can be utilized in cosmetology and medical treatment as a peeling medicament, or even an antiseptic for drinking water. Therefore a fast and facile method to detect TCA is of essence and significance. Electrocatalytic behavior towards TCA on Nafion/HRP/Co_3O_4/CILE was performed with the results displayed in Fig.6. With TCA adding into pH 3.0 PBS, the cathodic response at -0.250 V was

increasing gradually while the anodic peak decreasing and disappeared at last. Meanwhile the second reduction peak appeared at -0.529 V at the higher TCA concentration, suggesting that a characteristic electrocatalysis took place [35]. And the electrocatalytic equations were shown as follows:

HRP Fe(III) + e → HRP Fe(II)

$2HRP\ Fe(II)+Cl_3CCOOH+H^+ \rightarrow 2HRP\ Fe(III)+Cl_2CHCOOH+Cl^-$

HRP Fe(II) + e → HRP Fe(I)

$2HRP\ Fe(I)+Cl_2CHCOOH+H^+ \rightarrow 2HRP\ Fe(II)+ClCH_2COOH+Cl^-$

$2HRP\ Fe(I)+ClCH_2COOH+H^+ \rightarrow 2HRP\ Fe(II)+CH_3COOH+Cl^-$

Reduction peak responses were enhanced proportionally with TCA concentration and the equation was I (μA) = 1.963 C (mmol·L^{-1}) + 3.897 (n=10, γ=0.997) in the TCA concentration ranging from 5.0 to 90.0 mmol·L^{-1} with the detection limit estimated to be 1.7 mmol·L^{-1} (3σ). When TCA concentration was higher than 90.0 mmol·L^{-1}, the catalytic current almost kept stable, exhibiting a Michaelis-Menten dynamic mechanism. The Lineweaver-Burk equation is used to evaluate enzymatic reaction [36]: $1/I_{ss} = 1/I_{max} + K_M^{app}/(I_{max} \cdot C)$ (I_{ss} is for the instantaneous current that be detected in detectable range; I_{max} is for the maximum current detected in saturated environment; C is for the concentration of substrate), by which the apparent Michaelis-Menten constant (K_M^{app}) [37] was calculated as 88.15 mmol·L^{-1}.

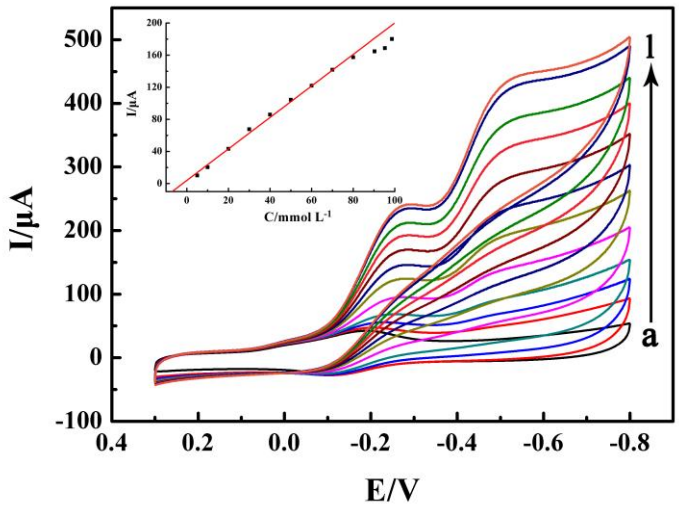

Figure 6. CVs of Nafion/HRP/Co_3O_4/CILE with different concentrations of TCA (from a to l as 0.0, 2.0, 5.0, 10.0, 20.0, 30.0, 40.0, 50.0, 60.0, 70.0, 80.0, 90.0 mmol·L^{-1}; inset is the linear relationship of TCA concentration versus cathodic current).

$NaNO_2$ contains food-borne toxicity and can turn into carcinogenic nitrosamine in living body, which can deprive the ability of oxygen transport in blood. Therefore it is necessary to establish a sensitive method for $NaNO_2$ detection. Electrocatalysis of Nafion/HRP/Co_3O_4/CILE towards $NaNO_2$ was further performed with results shown in Fig.7. A new reduction peak was observed at -0.725 V with the addition of $NaNO_2$ in PBS at $NaNO_2$ concentration ranged from 0.1 to 1.1 mmol·L^{-1}. A linear regression equation for $NaNO_2$ concentration versus cathodic current was got as I (μA) = 27.05 C (mmol·L^{-1}) + 39.69 (n=11, γ=0.993). The detection limit was 33 μmol·L^{-1} (3σ) and K_M^{app} was reckoned as 0.201 mmol·L^{-1}.

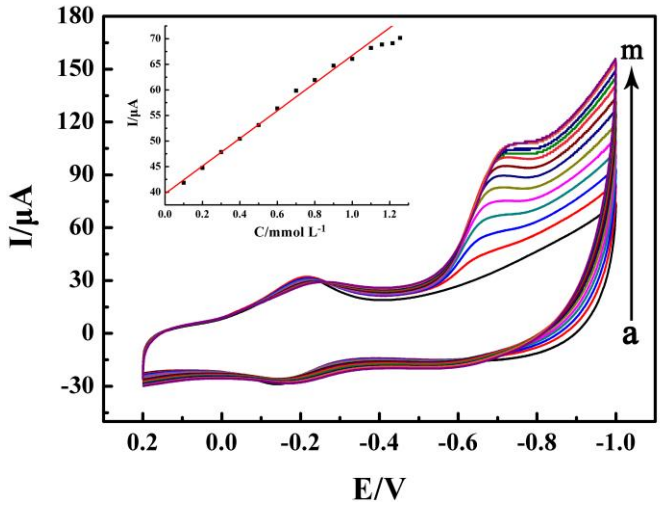

Figure 7. CVs of Nafion/HRP/Co_3O_4/CILE with different concentrations of $NaNO_2$ (from a to m as 0.0, 0.1, 0.2, 0.3, 0.4, 0.5, 0.6, 0.7, 0.8, 0.9, 1.0, 1.1, 1.2 mmol·L^{-1}; inset is the linear relationship of $NaNO_2$ concentration versus cathodic current).

3.7 Practical applications

Various samples containing TCA and $NaNO_2$ were analyzed by this proposed method. Medical facials peel (35% TCA, Shanghai EKEAR Bio. Tech. Ltd. Co., China) was diluted by pH 3.0 PBS and used for the determination of TCA. Pickled vegetables were brought from farm product market and the soak water was got by filtering dreg out of the mixture before usage for the determination of $NaNO_2$. The analyte existed in the sample solution and the concentration was calculated by the calibration curve. As shown in table 1, the analytical data was summarized and the recoveries were got by the standard addition method, which were from 96.70% to 99.15% for TCA and from 95.00% to 110.00% for $NaNO_2$, respectively, proving the real applications in different samples.

Table 1. Analytical data of TCA and $NaNO_2$ concentration in real samples by the proposed method (n=3)

Sample	Detected (mmol·L^{-1})	Added (mmol·L^{-1})	Total (mmol·L^{-1})	Recovery (%)
Medical facial peel solution for TCA	30.66	20.00	50.49	99.15
		40.00	69.34	96.70
		60.00	89.55	98.15
Soak water from pickled vegetables for $NaNO_2$	0.44	0.10	0.55	110.00
		0.20	0.63	95.00
		0.30	0.75	103.33

4. CONCLUSIONS

In this paper Co_3O_4 NPs were used to the realization of HRP direct electrochemistry with CILE. The fabrication of Nafion/HRP/Co_3O_4/CILE exhibited excellent electrocatalytic effects to the reduction of various substrates such as TCA and $NaNO_2$ with wider linear range and low detection limit. Real samples from drug and food were detected by this electrochemical biosensor with satisfactory results. Therefore Co_3O_4 NPs exhibits as an excellent candidate for the preparation of electrochemical enzyme sensors.

ACKNOWLEDGEMENTS
This project was financially supported by the National Natural Science Foundation of Hainan Province (2017CXTD007), the Key Science and Technology Program of Haikou City (2017042) and Foundation of Key Laboratory of Sensor Analysis of Tumor Marker of Ministry of Education of Qingdao University of Science and Technology (STAM201808).

References

1. S. Mittal, H. Kaur, N. Gautam and A.K. Mantha, *Biosens. Bioelectron.,* 88 (2017) 217
2. P. Biswas, A.K. Karn, P. Balasubramanian and P.G. Kale, *Biosens. Bioelectron.,* 94 (2017) 589
3. M.R. Saidur, A.R.A. Aziz and W.J. Basirun, *Biosens. Bioelectron.,* 90 (2017) 125
4. T.Y. Zhou, H.W. Han, P. Liu, J. Xiong, F.K. Tian and X.K. Li, *Sensors*, 17 (2017) 2230
5. H.X. Dai, W.J. Lü, X.W. Zuo, Q. Zhu, C.J. Pan, X.Y. Niu, J.J. Liu, H.L. Chen and X.G. Chen, *Biosens. Bioelectron.,* 95 (2017) 131
6. K.A. Razak, M.N. Noorhashimah and N.S. Ridhuan, *Advanced Materials and their Applications: Micro to nano scale, Chapter: Metal Oxide Nanostructure-modified Electrode for Glucose Biosensor*, One Central Press, (2017) Lancashire Manchester, the United Kingdom
7. Y.H. Wang, K.J. Huang and X. Wu, *Biosens. Bioelectron.,* 97 (2017) 305
8. S.C. Ray and N.R. Jana, *Carbon Nanomaterials for Biological and Medical Applications, Chapter 3: Application of Carbon-Based Nanomaterials as Biosensor, 1st edition*, Elsevier, (2017) Amsterdam, Netherlands
9. P. Suvarnaphaet and S. Pechprasarn, *Sensors*, 17 (2017) 2161
10. M.R. Saidur, A.R.A. Aziz and W.J. Basirun, *Biosens. Bioelectron.,* 90 (2017) 125
11. D.X. Yang, X.C. Liu, Y.Y. Zhou, L. Luo, J.C. Zhang, A.Q. Huang, Q.M. Mao, X. Chen and L. Tang, *Anal. Methods*, 9 (2017) 1976
12. N. Verma, A.K. Singh and M. Singh, *Biosens. Bioelectron.,* 12 (2017) 228
13. L. Bao, T. Li, S. Chen, C. Peng, L. Li, Q. Xu, Y.S. Chen, E.C. Ou and W.J. Xu, *Small*, 13 (2016) 1602077
14. L. Yu, P. Zhang, H.X. Dai, L. Chen, H.Y. Ma, M. Lin and D.Z. Shen, *RSC Adv.,* 7 (2017) 39611
15. C.R. Dhas, R. Venkatesh, D.D. Kirubakaran, J.P. Merlin, B. Subramanian, A. M.E. Raj, *Mater. Chem. Phys.,* 186 (2017) 561
16. C.Y. Song, X.Z. Yin, B.P. Li, K. Ye, K. Zhu, D.X. Cao, K. Cheng and G.L. Wang, *Dalton Trans.*, 46 (2017) 13845
17. S.Q. Cui, L. Li, Y.P. Ding and J.J. Zhang, *J. Electroanal. Chem.,* 782 (2016) 225
18. H. Liu, K. Guo, C.Y. Duan, X.J. Chen and Z.F. Zhu, *Mater. Sci. Eng. C*, 64 (2016) 243
19. R. Mohammad, M. Ahmad and L.Y. Heng, *Sens. Actuat. B-Chem.,* 241 (2017) 174

20. L. Wu, W.M. Yin, K. Tang, D. Li, K. Shao, Y.P. Zuo, J. Ma, J.W. Liu and H.Y. Han, *Anal. Chim. Acta*, 933 (2016) 89
21. Y.D. Liu, X.H. Liu , Z.P. Guo, Z.A. Hu, Z.H. Xue and X.Q. Lu, *Biosens. Bioelectron.*, 87 (2017) 101
22. Q.Q. Ren, J. Wu, W.C. Zhang, C. Wang, X. Qin,G.C. Liu, Z.X. Li and Y. Yu *Sens. Actuat. B-Chem.*, 245 (2017) 615
23. W. Chen, X.L. Niu, X.Y. Li, X.B. Li, G.J. Li, B.L. He, Q.T. Li and W. Sun, *Mater. Sci. Eng. C*, 80 (2017) 135
24. M.F. Valan, A. Manikandan and S.A. Antony, *J. Nanosci. Nanotechnol.*, 15 (2015) 4580
25. V.G. Hadjiev, M.N. Iliev and I.V. Vergilov, *J. Phys. C: Solid State Phys.*, 21 (1988) L199
26. J. Yang, H.W. Liu, W.N. Martens and R.L. Frost, *J. Phys. Chem. C*, 114 (2010) 111
27. K. Rosenheck and P. Doty, *PNAS*, 47 (1961) 1775
28. D.M. Byler and H. Susi, *Biopolymers*, 25(1986) 469
29. W. Zheng, W.S. Zhao, W. Chen, W.J. Weng, Z.W. Liao, R.X. Dong, G.J. Li and W. Sun, *Int. J. Electrochem. Sci.*, 12 (2017) 4341
30. X.Y. Li, X.l. Niu, W.S. Zhao, W. Chen, C.X. Yin, Y.L. Men, G.J. Li and W. Sun, *Electrochem. Commun.*, 86 (2018) 68
31. A.J. Bard and L.R. Faulkner, *Electrochemical Methods, Fundamentals and Applications, 2ed edition*, Wiley, (2001) New York, the United States of America
32. F. Shi, W.Z. Zheng, W.C. Wang, F. Hou, B.X. Lei, Z.F. Sun and W. Sun, *Biosens. Bioelectron.*, 64 (2015) 131
33. F. Shi, J.W. Xi, F. Hou, L. Han, G.J. Li, S.X. Gong, C.X. Chen and W. Sun, *Mater. Sci. Eng. C*, 58 (2016) 450
34. W. Zheng, G.J. Li, L.H. Liu, W. Chen, W.J. Weng and W. Sun, *Int. J. Electrochem. Sci.*, 11 (2016) 7584
35. D.P. Qian, W.B. Li, F.T. Chen and C.M. Yu, *Microchim. Acta*, 184 (2017) 1977
36. R.A. Kamin and G.S. Wilson, *Anal. Chem.*, 52 (1980) 1198
37. X.L. Wang, L.H. Liu, W. Zheng, W. Chen, G.J. Li and W. Sun, *Int. J. Electrochem. Sci.*, 11 (2016) 1821